Accuracy of Predicting the Moisture Content of Three Types of Wood Sections Using Near Infrared Spectroscopy

Yohei Kurata *

The moisture content of wood affects its physical properties. Many researchers have attempted to measure wood moisture contents nondestructively using near-infrared (NIR) spectroscopy. Wood is a natural material with anisotropic characteristics. There are three section types of cut wood surfaces, namely cross, radial, and tangential sections. In this study the NIR spectra of all three types of wood sections were measured and compared to determine how accurately the water content of softwood could be predicted. Two wood species were chosen and were cut into 30-mm cubes. The wood samples were stored for two weeks under various humidity conditions before they underwent NIR spectroscopy. The NIR spectra were obtained from three wood sections and principal component regression (PCR) was performed. Good calibration models for the three types of sections were then obtained. Furthermore, to expand the application of the PCR model for each section type, combinations of calibration models and prediction sets of the other sections were implemented. For the cross section models, there was no clear prediction capability when the test sets from the other two section types were used. However, for the radial and tangential sections, a high prediction accuracy was obtained using the other test set.

Keywords: Wood water content; Near-infrared spectroscopy; Principal component regression; Japanese cypress; Douglas fir

*Contact information: College of Bioresource Sciences, Nihon University, 1866 Kameino, Fujisawa, Kanagawa 252-0880, Japan; *Corresponding author: kurata.youhei@nihon-u.ac.jp*

INTRODUCTION

Near-infrared (NIR) spectroscopy is widely used to nondestructively analyze the moisture content of various foods, including vegetables and fruits, and other agricultural commodities (Rodriguez-Otero *et al*. 1997; Büning-Pfaue 2003; Andrés *et al*. 2007). The relationship between the NIR spectra region and water absorption band has been extensively studied (Langford *et al*. 2001; Segtnan *et al*. 2001). It is important to predict the moisture content for grading and qualifying commodities. Furthermore, as water molecules adopt a complex structure because of intermolecular hydrogen bonding, the number of hydrogen bonds and the behavior of molecular clusters can be measured and estimated using NIR spectroscopy (Adachi *et al*. 2002). In the case of wood, it is also vital to measure the water content inside of the material. The water content in wood has been examined in detail using modern and archaeological wood samples combined with spectral decomposition related to the absorption of NIR light (Inagaki *et al*. 2008).

The moisture content affects the physical properties of wood. For instance, the compression and bending strengths decrease as the moisture content increases to approximately 30%; above 30%, the compression and bending strengths are constant

(Kollman and Côté Jr. 1968). Measurement of the wood moisture content is of great advantage to ensure the wood quality. Many researchers have attempted to measure wood moisture contents nondestructively using NIR spectroscopy with good predictability (Roy *et al*. 1993; Uddin *et al*. 2006). When possible, physical properties that change according to the moisture content are measured one at a time. Wood is a natural material with anisotropic characteristics. There are three section types of cut wood surfaces, which are cross, radial, and tangential sections. Near-infrared spectroscopy of wood samples is mostly performed on tangential and radial surfaces (Schimleck *et al*. 2003; Fujimoto *et al*. 2008). Thus, differences in the NIR spectra obtained from these three surface types have not been compared to assess the accuracy of predicting the moisture content using NIR spectroscopy.

In this study, a multivariate analysis of the NIR spectra to nondestructively measure the water content of softwood was used. The prediction accuracies of the NIR regression results obtained from all three types of wood surfaces were compared. Furthermore, calibration models obtained from each section type were evaluated to determine if they could be applied to the other surfaces, thus providing fundamental data on the wood sections and their moisture-related behavior.

EXPERIMENTAL

Materials

Wood sample preparation

Samples from two wood species (*Chamaecyparis obtusa* (Japanese cypress) and *Pseudotsuga menziesii* (Douglas fir)) were prepared and cut into 30-mm cubes. Two samples of each section type (cross, tangential, and radial) were used and the measured spectral data was averaged between the two sections. The sample size and sensor area are shown in Fig. 1.

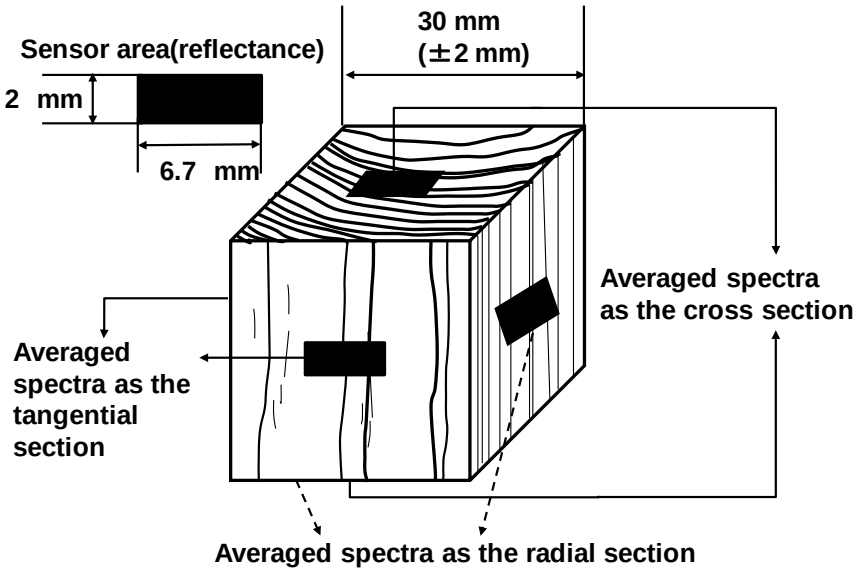

Fig. 1. Outline of the sample surface and NIR measurement area

In all, three different pieces of NIR data were measured for each specimen. The radial sections were defined as having an annual ring angle of less than 15°. Furthermore, because the cross section samples from the cutting process had a fuzzy surface that scattered light when cut with a band saw, the surface was smoothed with an end surface cutter (cutting machine D type, Fujikyu Machinery Industry, Nagoya, Japan). The cutting error was within 2 mm.

Methods

Storage conditions and moisture content measurement

After cutting, the samples were stored for two weeks in a thermo-hygrostat (THE051FA, Toyo Engineering Works Advantec, Kashiwa, Japan), which is a constant low temperature humidity chamber. The humidity conditions varied from 0% to 90% at 23 °C ± 0.5 °C. The humidity conditions and approximate wood moisture contents are summarized in Table 1. Total measurement sample number for *C. obtusa* and *P. menziesii* were 130 and 109, respectively. Though low humidity conditions were of interest, the wood surface was saturated with water at a high humidity. The low water content was measured around the fiber saturation point. The moisture content was calculated by dividing the water content with the dry wood sample weight.

Table 1. Outline of the Sample Numbers for Each Humidity Condition

Relative Humidity (%)	Approximate Water Content (%)	Sample Number (Calibration set number)	
		C. obtusa	*P. menziesii*
0	0 - 2	20 (15)	29 (21)
30	8 - 9	40 (30)	10 (6)
70	10 - 13	30 (25)	30 (22)
90	15 - 20	40 (30)	40 (30)
Total		130 (100)	109 (79)

NIR measurement procedure

The NIR spectrometer measured the wavelength range from 1200 nm to 2500 nm (S-7100, Soma Optics Ltd., Tokyo, Japan). The resolution used was 1.0 nm. The samples were first irradiated with a monochromatic light and the reflectance (five-scan average) was obtained. First, the NIR spectra measured from each section of the wood samples stored in the humidity chamber were measured. After the NIR measurement, the wood samples were dried and the water contents were calculated. The relationship between the NIR spectral data and wood water content was examined using multivariable data analysis.

Data pre-processing

The statistics for the water content measurements of the calibration and prediction sample sets are summarized in Table 2. The calibration set was used to build the regression model, and the prediction set was used for comparison of the prediction accuracy. The calibration set included the high and low water content values.

The average and standard deviations were almost the same for each sample of the calibration and prediction sets. The detailed numbers for the calibration set are shown in Table 1. The raw NIR spectra often exhibited a baseline shift or drift because of variations in the measurement. Moreover, various factors can affect the NIR spectrum, such as the instrument stability, temperature, humidity, and surface conditions of the sample (Candolfi *et al*. 1999). Therefore, data pretreatment is an important step to reduce errors during data analysis.

The pretreated NIR spectra (moving average smoothing with segment size 13; multiplicative scatter correction; and second derivative with segment size 13) were used for this analysis (Fujimoto *et al*. 2010; Kurata 2017). Moving average smoothing eliminated random noise from the NIR spectra. Multiplicative scatter correction compensated for both multiplicative and additive effects on the spectra. The second derivative also reduced multiplicative and additive effects and amplified peaks buried in the spectra.

Principal component regression (PCR) was performed. The final number of factors used for each calibration was recommended by the Unscrambler X software (version 10.1, Camo Software, Oslo, Norway). The data was evaluated based on the correlation coefficient (R^2 for the calibration set and R_p^2 for the prediction set) between the predicted and measured values. Additionally, the statistics root mean square error of the cross validation (RMSECV) and root mean square error of the prediction (RMSEP) were evaluated and compared for the calibration and prediction sets (Williams and Sobering 1993; Schimleck *et al*. 2001, 2003; Fujimoto *et al*. 2010).

Table 2. Outline of the Wood Sample Number and the Water Content Statistical Values in the Calibration and Prediction Set

Species	Calibration Set					Prediction Set				
	n	Min. (%)	Max. (%)	Ave. (%)	SD	*n*	Min. (%)	Max. (%)	Ave. (%)	SD
C. obtusa	100	0.51	18.2	10.5	5.3	30	0.61	17.2	10.4	5.6
P. menziesii	79	0.39	20	11.3	7.1	30	0.49	19.4	10.9	7

n - sample number; Min.- minimum; Max. – maximum; Ave. - average; and SD - standard deviation

RESULTS AND DISCUSSION

Table 3 shows the PCR results for the water content predictions using the pretreated NIR spectra. In the calibration results, the R^2 values ranged from 0.93 to 0.96 and the RMSECV ranged from 0.82 to 1.01. In the prediction results, the R_p^2 values ranged from 0.86 to 0.93 and the RMSEP ranged from 0.75 to 0.97. This meant that good calibration models were obtained for the three section types measured. There were no differences in the PCR results between the wood species or section types.

Table 3. PCR Results for the Water Content Prediction Using the Pretreated NIR Spectra

Species	Section	Factors	R^2	RMSECV	R_p^2	RMSEP
C. obtusa	Cross section	3	0.93	0.99	0.88	0.85
	Radial section	3	0.95	0.83	0.89	0.75
	Tangential section	3	0.95	0.82	0.90	0.82
P. menziesii	Cross section	3	0.94	0.98	0.86	0.75
	Radial section	3	0.96	0.87	0.93	0.87
	Tangential section	3	0.95	1.01	0.90	0.97

Figure 2 shows the regression coefficients for the PCR models predicting the water content based on the calculations from the pretreated NIR spectra.

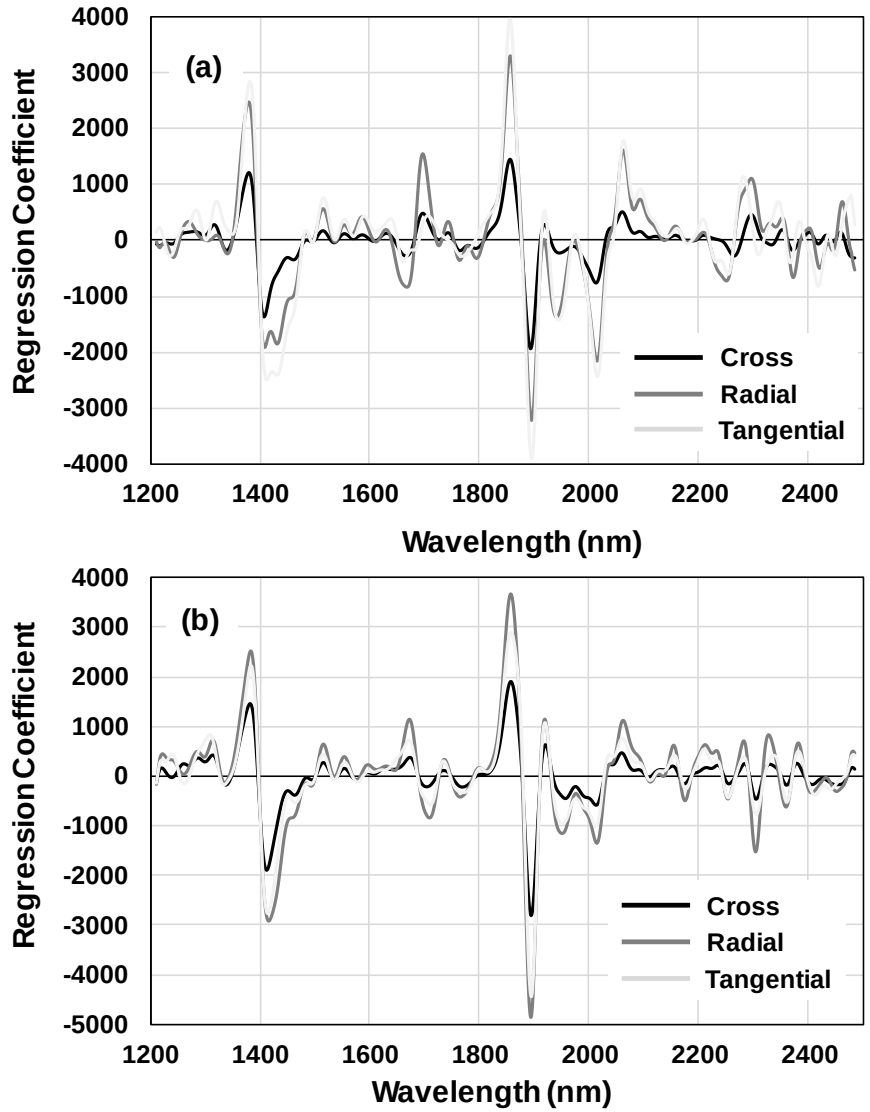

Fig. 2. Regression coefficients for the PCR models predicting the water content calculated from the pretreated NIR spectra with (a) *C. obtusa* and (b) *P. menziesii*

The cross section measurements differed slightly from the other two section types for both wood species. Schwanninger *et al*. (2011) extensively examined the NIR spectral band assignments for major wood components in the NIR region from approximately 1000 nm to 2500 nm. The water band locations in the wood sections were assigned to 1414 nm (first overtone O-H stretching vibration), 1916 nm to 1942 nm (combination band between O-H antisymmetric stretching vibration and O-H deformation vibration of H_2O), and 1980 nm (combination band between O-H stretching vibration and O-H deformation vibration of H_2O). High negative and positive regression coefficients were observed in these regions.

The explained variances of the first three PCR factors derived from each model are given in Table 4. The Explained X indicates how much the PCR factor could explain the deviation of the NIR spectra, whereas the Explained Y shows the deviation in the wood water content. In the cross sections, the first PCR values were lower than that for other sections and the second PCR values were higher.

Table 4. Explained Variances of the First Three PCR Factors Derived from Each Model

Species	Number of Factors	Cross Section		Radial Section		Tangential Section	
		Exp. X (%)	Exp. Y (%)	Exp. X (%)	Exp. Y (%)	Exp. X (%)	Exp. Y (%)
C. obtusa	1	95.6	83.6	96.9	85.1	97.4	84.6
	2	4.1	13.9	2.9	13.1	2.4	13.4
	3	0.2	1.9	0.1	1.4	0.1	1.6
P. menziesii	1	92.1	79.9	94.2	83.9	94.6	81.9
	2	7.6	17.9	5.6	13.8	5.2	15.9
	3	0.2	1.6	0.1	2.0	0.1	1.6

Exp. - explained

Figure 3 shows the loading plots for the three PCR factors used for predicting the water content with the pretreated NIR spectra of *C. obtusa*. The loading plots of factor 1 were almost the same shape for all three section types, while factors 2 and 3 differed slightly for the cross sections.

Figure 4 shows the loading plots for *P. menziesii*. The loading plots of all three sections exhibited almost the exact same trends (same shape).

Table 5 shows the PCR results for combinations between the calibration and prediction sets of the other wood sections. The combination between the calibration and prediction sets for the same section type showed a high prediction accuracy in accordance with the results in Table 3. With the cross section models, there was no clear prediction capability for the other two section types. However, with the radial and tangential section models, high prediction accuracies were obtained when using the other prediction set. This tendency was observed for both wood species studied. Similarities between the radial and tangential sections in the wood fiber direction were also observed, in contrast to the cross sections. When evaluating the predictions of the water content in the wood, the cross sections should be separated from the other section types. The reason that the results from the cross sections could not be applied to the other models might have been the different orientation of the cell structure.

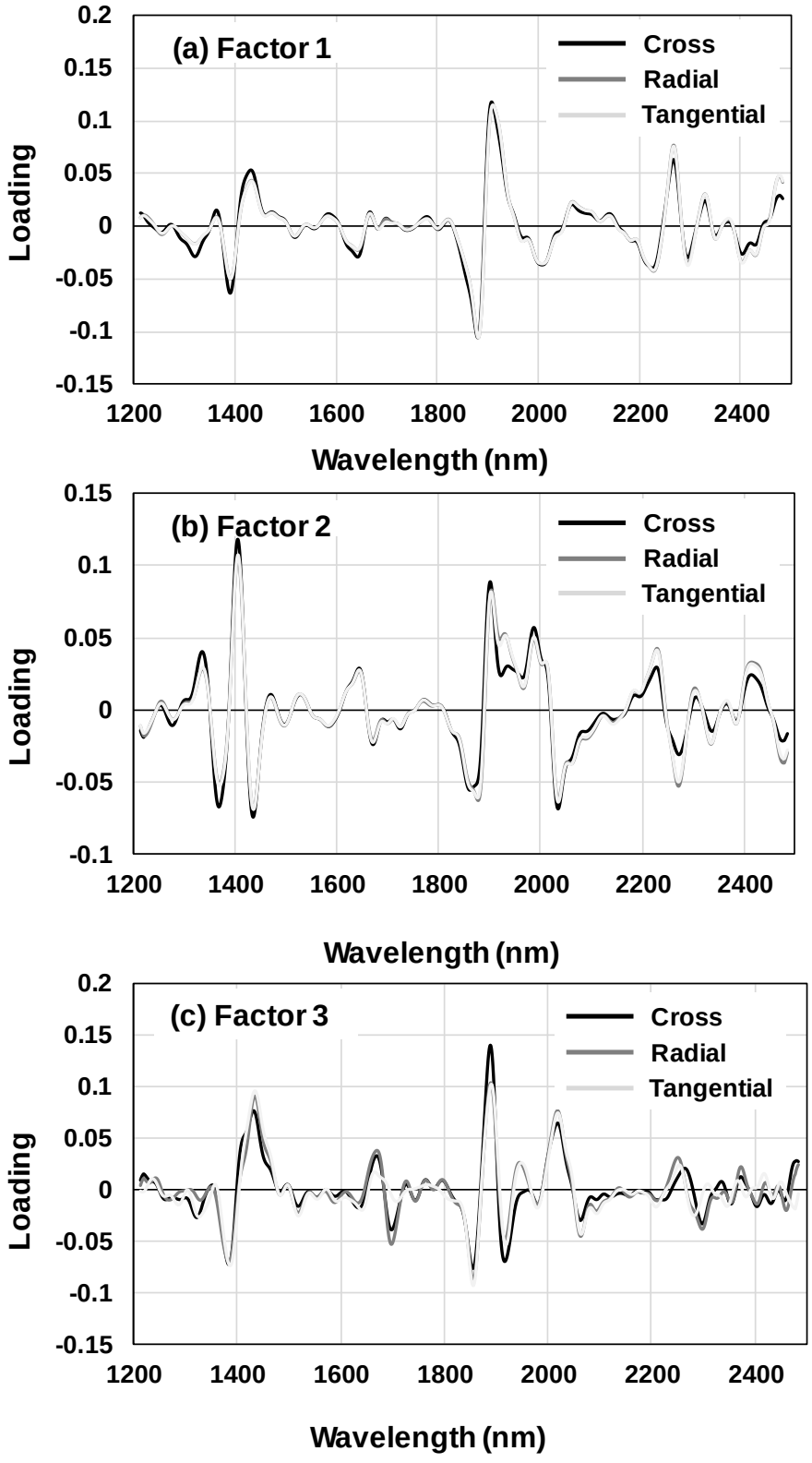

Fig. 3. Loadings for (a) factor 1, (b) factor 2, and (c) factor 3 for predicting the water content calculated from the pretreated NIR spectra with *C. obtusa*

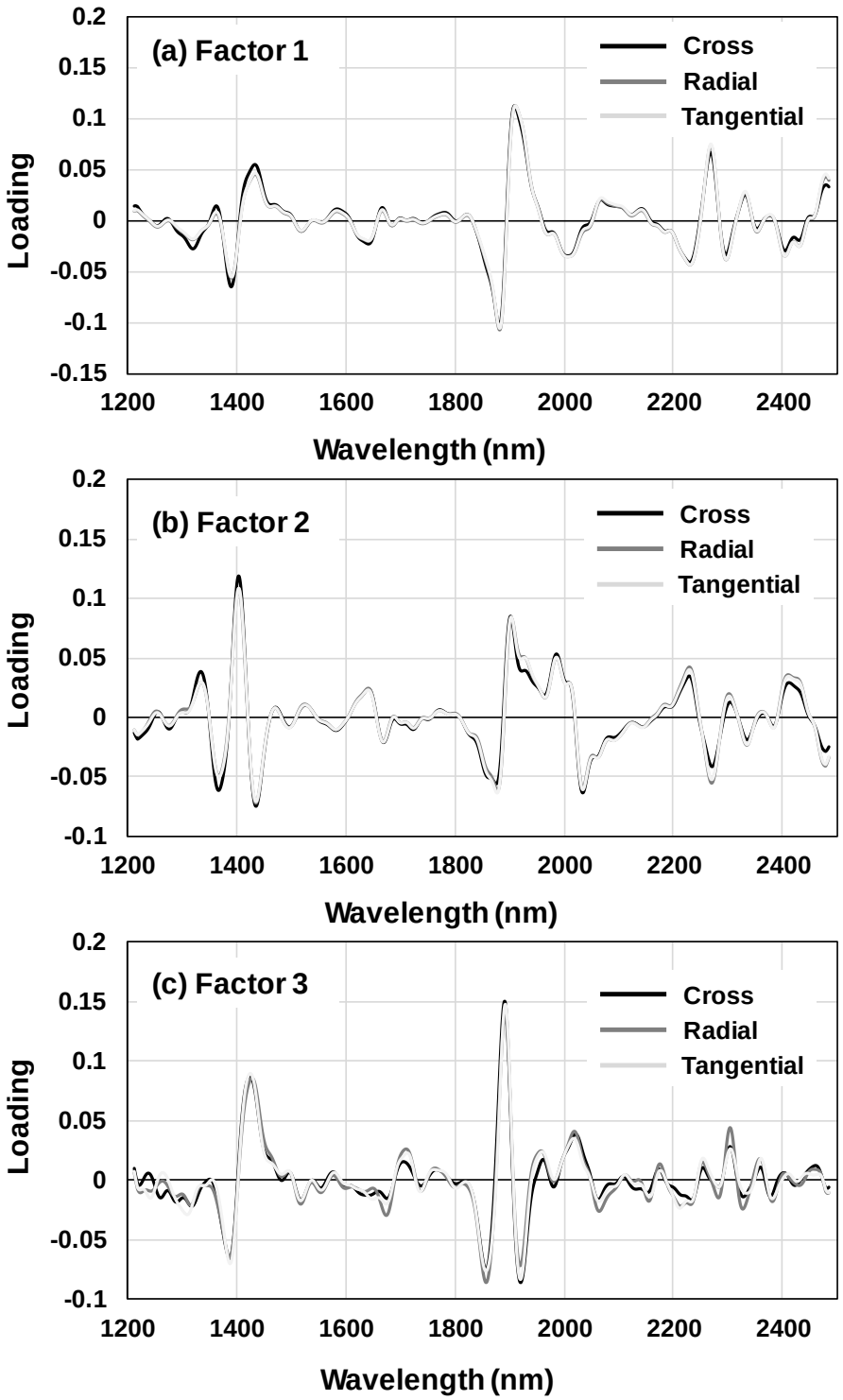

Fig. 4. Loadings for (a) factor 1, (b) factor 2, and (c) factor 3 for predicting the water content calculated from the pretreated NIR spectra with *P. menziesii*

Wood material obtained by end grain cutting rarely has practical uses. However, boards cut in the radial and tangential directions have more general uses. Thus, the calibration model from the boards cut in the radial and tangential directions, instead of the cross sections, was sufficient to predict the water content. Schimleck *et al*. (2018)

compared the NIR spectroscopy method for estimating wood mechanical properties from different wood surface (radial and cross section). As they focused on two sections for research, it corresponded approximately to this result.

However, in this study, a low moisture content was measured because of the limitations of the storage chamber. However, another problem was that a difference in the water content near the surface and in the interior of the wood board occurred during the drying process. Hence, a technique to monitor the drying process starting from a high water content should be developed. Furthermore, as softwood samples were used in this study, new insights might be obtained by examining the variations in wood types other than softwood.

Table 5. PCR Results for the Combination Between the Training and Test Sets

Species	Training Set (PCR)	Test Set	R_p^2	RMSEP
C. obtusa	Cross section	Cross section	0.88	0.85
		Radial section	ND	ND
		Tangential section	ND	ND
	Radial section	Cross section	ND	ND
		Radial section	0.89	0.75
		Tangential section	0.82	1.19
	Tangential section	Cross section	ND	ND
		Radial section	0.84	1.11
		Tangential section	0.90	0.82
P. menziesii	Cross section	Cross section	0.86	0.75
		Radial section	0.38	5.40
		Tangential section	0.40	5.29
	Radial section	Cross section	ND	ND
		Radial section	0.93	0.87
		Tangential section	0.91	0.95
	Tangential section	Cross section	ND	ND
		Radial section	0.88	0.96
		Tangential section	0.90	0.97

ND - non-data (under the measurable limit)

CONCLUSIONS

1. This study demonstrated that NIR spectroscopy could be applied to predict the moisture content of softwood. Two wood species, Japanese cypress and Douglas fir, were used to evaluate the accuracy of predicting the wood moisture content by obtaining the NIR spectra from wood sections with three different orientations.
2. The wood samples were stored in a constant low temperature humidity chamber for two weeks, until the wood water content was constant inside of the wood. The humidity was then changed, and the water content showed some variation at the fiber saturation point. The PCR technique was used for regression analysis of the pretreated spectra, which yielded good calibration models and predictions for all three wood section types.
3. The regression coefficient obtained by PCR changed at approximately 1450 nm and 1950 nm, which matched the water absorption band. The loading plots were found to be the same.
4. A PCR analysis for combinations between the calibration and prediction sets of the other wood section types was performed. Both the radial and tangential sections had a high prediction accuracy when using the other prediction set, but the cross section did not have a high accuracy when using the radial or tangential prediction sets. Therefore, a separate PCR model should be used for predicting the water content from the cross section. In practice, this means calibration using spectral data to predict the water content in wood should be based on the wood section type used.

REFERENCES CITED

Adachi, D., Katsumoto, Y., Sato, H., and Ozaki, Y. (2002). "Near-infrared spectroscopic study of interaction between methyl group and water in water—methanol mixtures," *Appl. Spectrosc.* 56(3), 357-361. DOI: 10.1366/0003702021954728

Andrés, S., Murray, I., Navajas, E. A., Fisher, A. V., Lambe, N. R., and Bünger, L. (2007). "Prediction of sensory characteristics of lamb meat samples by near infrared reflectance spectroscopy," *Meat Sci.* 76(3), 509-516. DOI: 10.1016/j.meatsci.2007.01.011

Büning-Pfaue, H. (2003). "Analysis of water in food by near infrared spectroscopy," *Food Chem.* 82(1), 107-115. DOI: 10.1016/S0308-8146(02)00583-6

Candolfi, A., Maesschalck, R. D., Massart, D. L., Hailey, P. A., and Harrington, A. C. E. (1999). "Identification of pharmaceutical excipients using NIR spectroscopy and SIMCA," *J. Pharmaceut. Biomed.* 19(6), 923-935. DOI: 10.1016/S0731-7085(98)00234-9

Fujimoto, T., Kurata, Y., Matsumoto, K., and Tsuchikawa, S. (2008). "Application of near infrared spectroscopy for estimating wood mechanical properties of small clear and full length lumber specimens," *J. Near Infrared Spec.* 16(6), 529-537. DOI: 10.1255/jnirs.818

Fujimoto, T., Kurata, Y., Matsumoto, K., and Tsuchikawa, S. (2010). "Feasibility of near-infrared spectroscopy for online multiple trait assessment of sawn lumber," *J. Wood Sci.* 56(6), 452-459. DOI: 10.1007/s10086-010-1122-5

Inagaki, T., Yonenobu, H., and Tsuchikawa, S. (2008). "Near-infrared spectroscopic monitoring of the water adsorption/desorption process in modern and archaeological wood," *Appl. Spectrosc.* 62(8), 860-865. DOI: 10.1366/000370208785284312

Kollman, F. F. P., and Côté Jr., W. A. (1968). "Electrical properties of wood," in: *Principles of Wood Sciences and Technology I Solid Wood*, Springer-Verlag, Berlin, Germany, pp. 257-273.

Kurata, Y. (2017). "Nondestructive classification analysis of wood soaked in seawater by using near-infrared spectroscopy," *Forest Prod. J.* 67(1-2), 63-68. DOI: 10.13073/FPJ-D-15-00049

Langford, V. S., McKinley, A. J., and Quickenden, T. I. (2001). "Temperature dependence of the visible-near-infrared absorption spectrum of liquid water," *J. Phys. Chem. A* 105(39), 8916-8921. DOI: 10.1021/jp010093m

Rodriguez-Otero, J. L., Hermida, M., and Centeno, J. (1997). "Analysis of dairy products by near-infrared spectroscopy: A review," *J. Agr. Food Chem.* 45(8), 2815-2819. DOI: 10.1021/jf960744p

Roy, S., Anantheswaran, R. C., Shenk, J. S., Westerhaus, M. O., and Beelman, R. B. (1993). "Determination of moisture content of mushrooms by vis–NIR spectroscopy," *J. Sci. Food Agr.* 63(3), 355-360. DOI: 10.1002/jsfa.2740630314

Schimleck, L. R., Evans, R., and Ilic, J. (2001). "Estimation of *Eucalyptus delegatensis* wood properties by near infrared spectroscopy," *Can. J. Forest Res.* 31(10), 1671-1675. DOI: 10.1139/x01-101

Schimleck, L. R., Mora, C., and Daniels, R. F. (2003). "Estimation of the physical wood properties of green *Pinus taeda* radial samples by near infrared spectroscopy," *Can. J. Forest Res.* 33(12), 2297-2305. DOI: 10.1139/x03-173

Schimleck, L. R., Matos, J. L. M., Trianoski, R., and Prata, J. G. (2018). "Comparison of methods for estimating mechanical properties of wood by NIR spectroscopy," *Journal of Spectroscopy* 10. DOI: 10.1155/2018/4823285

Schwanninger, M., Rodrigues, J. C., and Fackler, K. (2011). "A review of band assignments in near infrared spectra of wood and wood components," *J. Near Infrared Spec.* 19(5), 287-308. DOI: 10.1255/jnirs.955

Segtnan, V. H., Šašić, S., Isaksson, T., and Ozaki, Y. (2001). "Studies on the structure of water using two-dimensional near-infrared correlation spectroscopy and principal component analysis," *Anal. Chem.* 73(13), 3153-3161. DOI: 10.1021/ac010102n

Uddin, M., Okazaki, E., Fukushima, H., Turza, S., Yumiko, Y., and Fukuda, Y. (2006). "Nondestructive determination of water and protein in surimi by near-infrared spectroscopy," *Food Chem.* 96(3), 491-495. DOI: 10.1016/j.foodchem.2005.04.017

Williams, P. C., and Sobering, D. C. (1993). "Comparison of commercial near infrared transmittance and reflectance instruments for analysis of whole grains and seeds," *J. Near Infrared Spec.* 1(1), 25-32. DOI: 10.1255/jnirs.3

Article submitted: July 19, 2018; Peer review completed: September 9, 2018; Revised version received: September 13, 2018; Accepted: September 17, 2018; Published: September 26, 2018.
DOI: 10.15376/biores.13.4.8444-8454